Mixed Dual-Hop IRS-Assisted FSO-RF Communication System with H-ARQ Protocols

Gyan Deep Verma, Aashish Mathur, $Member, IEEE$, Yun Ai, $Member, IEEE$, and Michael Cheffena

***Abstract*—Intelligent reflecting surface (IRS) is an emerging key technology for the fifth-generation (5G) and beyond wireless communication systems to provide more robust and reliable communication links. In this letter, we propose a mixed dual-hop free-space optical (FSO)-radio frequency (RF) communication system that serves the end user via a decode-and-forward (DF) relay employing hybrid automatic repeat request (H-ARQ) protocols on both hops. Novel closed-form expressions of the probability density function (PDF) and cumulative density function (CDF) of the equivalent end-to-end signal-to-noise ratio (SNR) are computed for the considered system. Utilizing the obtained statistics, we derive the outage probability (OP) and packet error rate (PER) of the proposed system by considering generalized detection techniques on the source-to-relay (S-R) link with H-ARQ protocol and IRS having phase error. We obtain useful insights into the system performance through the asymptotic analysis which aids to compute the diversity gain. The derived analytical results are validated using Monte Carlo simulation.**

***Index Terms*—Free-space optical communication, decode-and-forward relaying, Gamma-Gamma turbulence, pointing errors, hybrid automatic repeat request.**

I. Introduction

In recent decade, free-space optical (FSO) communication systems have received significant attention in academic and industrial research thanks to their merits [1]. However, due to atmospheric turbulence (AT) and pointing error (PE), FSO communication system performance deteriorates. Various methods have been developed by researchers to overcome the effects of AT and PEs effectively, one of which is to use co-operative communication [1], [2]. A mixed dual-hop FSO-RF wireless communication system has been a promising solution for leveraging both wireless techniques to increase capacity, reduce power consumption, and extend wireless coverage by compensating the deteriorating effects of AT and PEs. To further improve the performance of the communication systems, hybrid automatic repeat request (H-ARQ) techniques can be utilized, which combines forward error correction (FEC) with re-transmission request protocols [3]. The approximate packet error rate (PER) of an RF communication system using H-ARQ with chase combining (CC) protocol was obtained in [4], [5]. The authors in [6], computed the outage probability (OP) and throughput performance of FSO communication systems employing various H-ARQ protocols under the combined influence of Gamma-Gamma (GG) distributed AT and PEs.

The intelligent reflecting surface (IRS) or meta-surfaces have been extensively explored in the literature, for their merits such as, capability of the greater coverage, improved spectrum and energy efficiency [1], [7]–[9]. In [1], the authors reported OP and BER performance for an IRS-aided dual-hop FSO-RF communication system. An IRS-assisted dual-hop mixed FSO-RF communication system was recently proposed in [7] where the OP and BER performance under the influence of co-channel interference (CCI) were evaluated. The authors in [8] performed OP analysis for an RF communication system using the H-ARQ with CC protocol over an IRS assisted with perfect phase estimation. However, the effect of phase errors in IRS was not considered in the aforementioned works.

Motivated by the recent studies on mixed FSO-RF communication systems using IRS and the benefits of H-ARQ protocols to improve the reliability of communication systems, we study the performance of an IRS-assisted mixed dual-hop FSO-RF communication system with H-ARQ protocols in this work. To the best of the authors' knowledge, such a cascaded system employing H-ARQ protocols over both links has not been investigated in literature. The following are the key contributions of our research work:

1) We derive closed-form expression of the probability density function (PDF) and cumulative distribution function (CDF) of the accumulated signal-to-noise ratio (SNR) with imperfect IRS phase estimation and H-ARQ protocol. Furthermore, using these expressions, we calculate the theoretic information OP and PER for the considered system.
2) We analyze the impact of various system parameters such as the number of IRS reflecting plates, number of transmission rounds, von Mises distribution concentration parameter (i.e., phase estimation accuracy of the IRS system), and packet length on the OP and PER performance which provide significant design insights into the considered system.
3) Useful insights into the system performance are obtained through the asymptotic expression of the OP.

II. System Description

We consider a cascaded dual-hop FSO-RF communication system where H-ARQ technique is employed on both the links. We assume that a source node (S) communicates with a destination node (D) via intermediary DF based relay (R). Due to obstructions caused by high-rise buildings and other impediments, it is justified that there is no direct path between source-to-destination (S-D) and relay-to-destination (R-D)

Gyan Deep Verma and Aashish Mathur are with the Department of Electrical Engineering, Indian Institute of Technology Jodhpur, Jodhpur, 342037, India (e-mails: {verma.11, aashishmathur}@iitj.ac.in).

Yun Ai and Michael Cheffena are with the Norwegian University of Science and Technology (NTNU), 7491 Trondheim, Norway (e-mail: yun.ai@ntnu.no; michael.cheffena@ntnu.no).

This work was supported in part by the Science and Education Research Board (SERB), Department of Science and Technology, Government of India for the Project "Experimental Investigation and Performance Evaluation of H-ARQ Technique for Free-Space Optical Communication Systems" (Project File No. ECR/2018/000797).

This article has been accepted for publication in a future issue of this journal, but has not been fully edited. Content may change prior to final publication. Citation information: DOI 10.1109/LCOMM.2021.3129594, IEEE Communications Letters

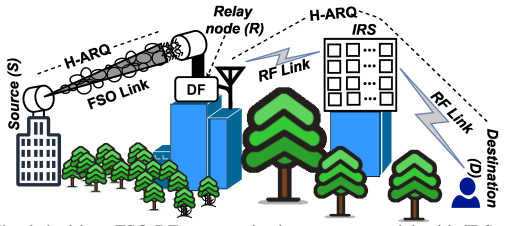

Fig. 1: Mixed dual-hop FSO-RF communication system model with IRS and H-ARQ protocol.

[1]. Hence, IRS is utilized on the RF link (R-D). The S-R link is a FSO link that is subjected to GG AT and PEs, which is widely used in the literature [1], [6], [7], [10]. For the FSO signal reception, both the heterodyne detection (HD) and intensity modulation and direct detection (IM/DD) techniques can be used. Rician and Rayleigh distributions are used on the RF hop between R-IRS and IRS-D, respectively, while von Mises distribution describes the phase shift errors of the IRS [11].

A. FSO Transmission Link

On the FSO communication link, we assume a single transmitter (Tx) and receiver (Rx) and use H-ARQ with CC protocol to enhance the system performance. The baseband electrical signal is represented after optical-to-electrical (O-E) conversion as follows:

$$y_{SR} = \eta_e s_1 h + w_R, \tag{1}$$

where η_e is the effective O-E conversion coefficient and the transmitted optical signal is s_1. The FSO channel gain is represented as h=$h_l h_a h_p$, where h_l denotes path loss [12], h_a signifies AT, and h_p indicates PE [13]. It is assumed that the transmitted power is $\mathbb{E}[s_1]$=P_1, where $\mathbb{E}[.]$ is the expectation operator, $w_R \sim \mathcal{CN}(0,\sigma_R^2)$ denotes the complex additive white Gaussian noise (AWGN) with zero mean and variance σ_R^2 at the relay node. The composite PDF of the received irradiance at the relay in the q^{th} round is expressed as [10, Eq. (8)],

$$f_{h_{SR_q}}(h_q) = \frac{ab\xi^2}{A_0 h_q \Gamma(a)\Gamma(b)} G_{1,3}^{3,0}\left(\frac{abh_q}{A_0}\middle| \begin{matrix}\xi^2+1\\ \xi^2, a, b\end{matrix}\right). \tag{2}$$

In (2), $G_{u,v}^{s,t}\left(z\middle| \begin{matrix}c_1,\ldots,c_u\\ d_1,\ldots,d_v\end{matrix}\right)$ represents the Meijer G-function [14, Eq. (9.301)] and $\Gamma(.)$ denotes the Gamma function [14, Eq. (8.31)]. The system parameters a, b, and ξ^2 are discussed in depth in [10]. After N_1 independent and identical H-ARQ transmission rounds over the S-R link, the random variable (RV) for the accumulated SNR is Z_{SR}=$\sum_{q=1}^{N_1}\gamma_{SR_q}$, where γ_{SR_q}=$(\eta_e h_q)^r/\sigma_R^2$ represents the instantaneous SNR on the S-R link in the q^{th} round and r=$\{1,2\}$ denotes HD and IM/DD, respectively. Further, using [10, Eq. (26)], the PDF of the RV Z_{SR} is written as

$$f_{Z_{SR}}(z) = \sum_{\substack{l_1+l_2+l_3=N_1\\ 0\le l_1,l_2,l_3\le N_1}} \binom{N_1}{l_1,l_2,l_3} \sum_{n=0}^{\infty} \frac{D_n(l_1,l_2,l_3) z^{\frac{E}{r}-1}}{\Gamma\left(\frac{E}{r}\right)\bar{\gamma}_{SR_r}^{\frac{E}{r}}}, \tag{3}$$

where l_1, l_2, and l_3 represent non-negative indices in the multinomial expansion. In (3), the parameter $D_n(l_1,l_2,l_3)$=$\tilde{X}_0^{\,l_1}(\tilde{Y}_n^{\,(l_2)} * \tilde{Z}_n^{\,(l_3)})$ is defined in [10, Eq. (23)], $\bar{\gamma}_{SR_r}$=$(\eta_e E[h_q])^r/\sigma_R^2$, $E[h_q]$=$(A_0\xi^2)/(\xi^2+1)$, E=$n+l_1\xi^2+l_2 a+l_3 b$, $*$ denotes convolution, and $\tilde{Y}_n^{\,(l_2)}$ shows that $\tilde{Y}_n$ is convolved (l_2-1) times with itself. Moreover, by integrating (3) with respect to z, the CDF of the RV Z_{SR} is derived as

$$F_{Z_{SR}}(z) = \sum_{\substack{l_1+l_2+l_3=N_1\\ 0\le l_1,l_2,l_3\le N_1}} \binom{N_1}{l_1,l_2,l_3} \sum_{n=0}^{\infty} \frac{D_n(l_1,l_2,l_3) z^{\frac{E}{r}}}{\Gamma\left(\frac{E}{r}\right)\left(\frac{E}{r}\right)\bar{\gamma}_{SR_r}^{\frac{E}{r}}}. \tag{4}$$

Remark 1: If Malaga distribution is assumed for the FSO link, it can be expressed in terms of the Meijer G-function, and as a result the PDF becomes similar to GG AT. Thus, the analysis would be similar.

B. RF Transmission Link

We assume that the R-D link is an RF link that utilizes IRS with M identical antenna reflector plates that serve as an intermediary node between R and D (spaces between two plates are maintained at least half wavelength). The locations of the IRS as well as large enough spacing between the reflectors ensure that the channels are independent and identically distributed (IID) [9], [11]. The RF signal after reflection from the IRS and received at D is written as follows [11]:

$$y_{RD} = M\sqrt{\gamma_0}\left[\sum_{i=1}^{M} I_{1_i} I_{2_i} I_{3_i} e^{j\Theta_i}\right] s_2 + w_D, \tag{5}$$

where s_2 is the transmitted symbol from R to D and $\mathbb{E}[s_2]$=1, γ_0 represents the average SNR when single reflecting plate is present, I_{1_i}=$(d_1)^{-\nu/2}\alpha_i \exp(-j\theta_i)$ and I_{2_i}=$(d_2)^{-\nu/2}\beta_i \exp(-j\psi_i)$ are the channel gains of the R-RIS and RIS-D links, and ν is the path loss exponent. Further, d_1, θ_i, and α_i are the distance, phase shift, and the Rician fading channel on the R-IRS link, respectively [11]. Likewise, d_2, ψ_i, and β_i are the distance, phase shift, and the Rayleigh fading channel on the IRS-R link, respectively [11]. I_{3_i}=$\delta_i \exp(j\phi_i)$ is the reflection coefficient induced by the i^{th} IRS reflector, δ_i=1 [1], [7], [8], $\forall_i$ and $w_D \sim \mathcal{CN}(0,\sigma_D^2)$ denotes the complex AWGN with zero mean and σ_D^2 variance at node D. To make the analysis practical, we incorporate the phase deviations defined as θ_i+ψ_i-ϕ_i=Θ_i in our analysis, where Θ_i is randomly distributed over $[-\pi,\pi)$ and is modeled by the circular distribution [11], [15]. The combined PDF of the R-IRS and IRS-D channels for the j^{th} transmission round after incorporating phase shift errors is comparable to a direct channel with Nakagami distribution and is given by [11, Eq. (11-12)]

$$f_{|I_{RD_j}|}(x) = \frac{2m^m}{\Gamma(m)\mu^{2m}} x^{2m-1}\exp\left(-\frac{m}{\mu^2}x^2\right), \tag{6}$$

where $|I_{RD_j}|$=$\frac{1}{M}\sum_{i=1}^{M}|I_{1_i}||I_{2_i}||I_{3_i}|\exp(j\Theta_i)$, μ is the common mean of M complex variables, and m is the shaping parameter. The parameter m depends on M, $I_\vartheta(k)$, $E[I_{1_i}]$, and $E[I_{2_i}]$, where $I_\vartheta(k)$ represents modified Bessel function of the first kind of order ϑ, and k is concentration parameter of von Mises distribution [11, Eq. (12)], [15, Eq. (3.5.17-3.5.22)]. The instantaneous SNR of the j^{th} transmission round at D is γ_{RD_j}=$M\gamma_0|I_{RD_j}^2|$. Now, using (6), the PDF of the instantaneous SNR on the R-D link on the j^{th} H-ARQ round is computed as follows:

$$f_{\gamma_{RD_j}}(\gamma_{RD_j}) = \frac{m^m}{\Gamma(m)\bar{\gamma}_{RD}^m}\gamma_{RD_j}^{m-1}\exp\left(-\frac{m}{\bar{\gamma}_{RD}}\gamma_{RD_j}\right), \tag{7}$$

where $\bar{\gamma}_{RD}$=$M^2\gamma_0$. Let Z_{RD}=$\sum_{j=1}^{N_2}\gamma_{RD_j}$ represent the accumulated instantaneous SNR after N_2 independent and identical

This article has been accepted for publication in a future issue of this journal, but has not been fully edited. Content may change prior to final publication. Citation information: DOI 10.1109/LCOMM.2021.3129594, IEEE Communications Letters

H-ARQ transmission rounds at node D. Utilizing (7), the moment generating function (MGF) of the RV Z_{RD} is calculated as

$$\mathcal{M}_{Z_{RD}}(s) = m^{N_2}\Gamma(m)^{N_2}(s+(m/\bar{\gamma}_{RD}))^{-mN_2}. \quad (8)$$

Taking the inverse Laplace transform of (8) and after some algebra, the PDF of the RV Z_{RD} is obtained as

$$f_{Z_{RD}}(t) = \left(\frac{mt}{\bar{\gamma}_{RD}}\right)^{N_2} \frac{e^{\frac{mt}{\bar{\gamma}_{RD}}}}{(N_2m-1)!}. \quad (9)$$

Integrating (9), the CDF of Z_{RD} is derived as

$$F_{Z_{RD}}(t) = \frac{\bar{\gamma}_{RD}}{m}\frac{\Upsilon\left(\frac{mt}{\bar{\gamma}_{RD}}, N_2m-1\right)}{(N_2m+1)!}, \quad (10)$$

where $\Upsilon(.,.)$ is the lower incomplete Gamma function [14, Eq. (8.350)].

III. Performance Analysis

A. Equivalent end-to-end SNR

The CDF of the equivalent end-to-end SNR for the aforementioned communication system is given by [7, Eq. (13)]

$$\begin{aligned} F_{\gamma_{eq}}(\gamma) &= \Pr[\min(Z_{SR}, Z_{RD}) < \gamma] \\ &= \Pr(Z_{SR} < \gamma) + \Pr(Z_{RD} < \gamma) \\ &\quad - \Pr(Z_{SR} < \gamma)\Pr(Z_{RD} < \gamma). \end{aligned} \quad (11)$$

The PDF of the equivalent SNR is obtained by simply differentiating (11) as follows:

$$\begin{aligned} f_{\gamma_{eq}}(\gamma) &= f_{Z_{SR}}(\gamma) + f_{Z_{RD}}(\gamma) - f_{Z_{SR}}(\gamma)F_{Z_{RD}}(\gamma) \\ &\quad - F_{Z_{SR}}(\gamma)f_{Z_{RD}}(\gamma). \end{aligned} \quad (12)$$

The PDF of the equivalent SNR for the considered system is thus obtained by substituting (3), (4), (9), and (10) into (12).

B. OP Analysis

An information-theoretic outage occurs when the mutual information after N H-ARQ transmission rounds falls below the required threshold information rate (R). Hence, the OP of the considered communication system is given by

$$P_o = \Pr\{I_1 \le R, \ldots, I_N \le R\}, \quad (13)$$

where I_p, $1 \le p \le N$, denotes the instantaneous mutual information in the p^{th} round. In CC protocol, the mutual information is calculated using the accumulated SNR at the Rx after N transmission rounds as $I_{CC}(N) = \log_2\left(1+\sum_{p=1}^{N}\gamma_p\right)$ [3], [8]. Hence, the OP for H-ARQ with CC protocol after N rounds can be computed as

$$P_o = \Pr\left\{\log_2\left(1+\sum_{p=1}^{N}\gamma_p\right) \le R\right\} = \Pr\left\{\sum_{p=1}^{N}\gamma_p \le (2^R-1)\right\}. \quad (14)$$

Using (11) and (14), the end-to-end OP for the considered system is obtained as

$$P_{o,CC} = P_{o,SR} + P_{o,RD} - P_{o,SR}P_{o,RD}, \quad (15)$$

where $P_{o,SR}$ and $P_{o,RD}$ are the OP for H-ARQ with CC protocol on S-R and R-D link, respectively. Further, on substituting (4) and (10) into (15), the OP of the considered system is derived as

$$\begin{aligned} P_{o,CC} &= \sum_{\substack{l_1+l_2+l_3=N_1 \\ 0\le l_1,l_2,l_3\le N_1}} \binom{N_1}{l_1,l_2,l_3} \sum_{n=0}^{\infty} \frac{D_n(l_1,l_2,l_3)(2^R-1)^{\frac{E}{r}}}{\Gamma\left(\frac{E}{r}\right)\left(\frac{E}{r}\right)\bar{\gamma}_{SR_r}^{\frac{E}{r}}} \\ &+ \frac{\bar{\gamma}_{RD}}{m}\frac{\Upsilon\left(\frac{m(2^R-1)}{\bar{\gamma}_{RD}}, N_2m+1\right)}{(N_2m-1)!} - \frac{\Upsilon\left(\frac{m(2^R-1)}{\bar{\gamma}_{RD}}, N_2m+1\right)}{(N_2m-1)!} \\ &\times \frac{\bar{\gamma}_{RD}}{m} \sum_{\substack{l_1+l_2+l_3=N_1 \\ 0\le l_1,l_2,l_3\le N_1}} \binom{N_1}{l_1,l_2,l_3} \sum_{n=0}^{\infty} \frac{D_n(l_1,l_2,l_3)(2^R-1)^{\frac{E}{r}}}{\Gamma\left(\frac{E}{r}\right)\left(\frac{E}{r}\right)\bar{\gamma}_{SR_r}^{\frac{E}{r}}}. \end{aligned} \quad (16)$$

Remark 2: Although, Eq. (16) consists of an infinite series, the error converges rapidly for finitely small values of n (to the order of 10^{-5} at 25 dB SNR for $n = 4$), for HD and IM/DD techniques.

C. Average Packet Error Rate Analysis

In this section, we will derive the PER for the considered dual-hop system. The PER of H-ARQ with CC protocol for a long packet over slow block fading channel after the p^{th} transmission round can be written as [4, Eq. (2)]

$$\mathrm{PER} = \int_0^{\infty}\cdots\int_0^{\infty} Q_1\cdots Q_p f(\gamma_1)\cdots f(\gamma_p)\, d\gamma_1\cdots d\gamma_p, \quad (17)$$

where Q_i, $i \in (1,2,\cdots,p)$ is the instantaneous PER under AWGN, i.e., Q_i=$g(\gamma)$ shows a steep waterfall characteristic with threshold T_0, $g(\gamma \mid \gamma \le T_0) \approx 1$ and $g(\gamma \mid \gamma > T_0) \approx 0$. Further, T_0 is computed as T_0=$\int_0^{\infty} g(\gamma)d\gamma$. The value of the threshold T_0 is computed using [4, Eq. (4)], [16, Eq. (7)]. In this letter, we have used $T_0 = 10.5616$ for a packet length of 1024 bits. Hence the approximated PER is given by [4, Eq. (3)], [16, Eq. (6-7)]

$$\mathrm{PER} \approx \int_0^{T_0} f_{\gamma_{eq}}(\gamma)d\gamma = J_1 + J_2 - J_3 - J_4, \quad (18)$$

where J_1=$\int_0^{T_0} f_{Z_{SR}}(\gamma)d\gamma$, J_2=$\int_0^{T_0} f_{Z_{RD}}(\gamma)d\gamma$, J_3=$\int_0^{T_0} f_{Z_{SR}}(\gamma) \times F_{Z_{RD}}(\gamma)d\gamma$, and J_4=$\int_0^{T_0} F_{Z_{SR}}(\gamma)f_{Z_{RD}}(\gamma)d\gamma$. J_1 and J_2 are calculated by using (4) and (10), respectively. Moreover, J_3 is derived with help of (3) and (10) as follows:

$$\begin{aligned} J_3 &= \sum_{\substack{l_1+l_2+l_3=N_1 \\ 0\le l_1,l_2,l_3\le N_1}} \binom{N_1}{l_1,l_2,l_3} \sum_{n=0}^{\infty} \frac{D_n(l_1,l_2,l_3)}{\Gamma\left(\frac{E}{r}\right)\bar{\gamma}_{SR_r}^{\frac{E}{r}}} \frac{\bar{\gamma}_{RD}}{m} \\ &\quad \times \int_0^{T_0} \gamma^{\frac{E}{r}-1} \frac{\Upsilon\left(\frac{m\gamma}{\bar{\gamma}_{RD}}, N_2m+1\right)}{(N_2m-1)!}d\gamma. \end{aligned} \quad (19)$$

After some mathematical simplification, Eq. (19) is solved by using [17, Eq. (2.10.2.2)] as follows:

$$\begin{aligned} J_3 &= \sum_{\substack{l_1+l_2+l_3=N_1 \\ 0\le l_1,l_2,l_3\le N_1}} \binom{N_1}{l_1,l_2,l_3} \sum_{n=0}^{\infty} \frac{D_n(l_1,l_2,l_3)}{\Gamma\left(\frac{E}{r}\right)\bar{\gamma}_{SR_r}^{\frac{E}{r}}} \left(\frac{m}{\bar{\gamma}_{RD}}\right)^{mN_2} \\ &\times B(1,u)\ {}_2F_2\left(mN_2+1, u; mN_2+2, u+1; \frac{T_0m}{\bar{\gamma}_{RD}}\right). \end{aligned} \quad (20)$$

In (20), u=$E/r + N_2m + 1$, $B(.,.)$ is the Beta function [14, Eq. (8.380)], and ${}_2F_2(.,.;.,.;.)$ is the Hypergeometric function [14, Eq. (9.14.1)]. The integral J_4 is computed by using (4), (9), and [14, Eq. (8.31)] as

This article has been accepted for publication in a future issue of this journal, but has not been fully edited. Content may change prior to final publication. Citation information: DOI 10.1109/LCOMM.2021.3129594, IEEE Communications Letters

$$\text{PER} \approx \sum_{\substack{l_1+l_2+l_3=N_1 \\ 0\le l_1,l_2,l_3\le N_1}} \binom{N_1}{l_1,l_2,l_3} \sum_{n=0}^{\infty} \frac{D_n(l_1,l_2,l_3)(T_0)^{\frac{E}{r}}}{\Gamma\left(\frac{E}{r}\right)\left(\frac{E}{r}\right)\bar{\gamma}_{SR_r}^{\frac{E}{r}}} + \frac{\bar{\gamma}_{RD}}{m} \frac{\Upsilon\left(\frac{mT_0}{\bar{\gamma}_{RD}}, N_2m-1\right)}{(N_2m-1)!} - \sum_{\substack{l_1+l_2+l_3=N_1 \\ 0\le l_1,l_2,l_3\le N_1}} \binom{N_1}{l_1,l_2,l_3} \sum_{n=0}^{\infty} \frac{D_n(l_1,l_2,l_3)}{\Gamma\left(\frac{E}{r}\right)\bar{\gamma}_{SR_r}^{\frac{E}{r}}} \left(\frac{m}{\bar{\gamma}_{RD}}\right)^{mN_2}$$
$$\times B(1,u)\ {}_2F_2\left(mN_2+1,u;mN_2+2,u+1;\frac{T_0m}{\bar{\gamma}_{RD}}\right) - \sum_{\substack{l_1+l_2+l_3=N_1 \\ 0\le l_1,l_2,l_3\le N_1}} \binom{N_1}{l_1,l_2,l_3} \sum_{n=0}^{\infty} \frac{D_n(l_1,l_2,l_3)}{\Gamma\left(\frac{E}{r}\right)\left(\frac{E}{r}\right)} \left(\frac{\bar{\gamma}_{RD}}{m}\right)^{\frac{E}{r}+1} \Upsilon\left(\frac{mT_0}{\bar{\gamma}_{RD}}, u\right). \quad (22)$$

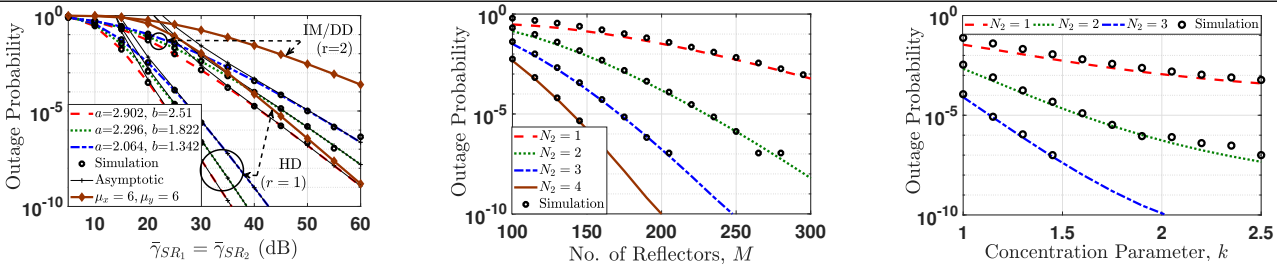

(a) (b) (c)

Fig. 2: Comparison of (a) OP versus SNR, (b) OP versus number of IRS reflectors, and (c) OP versus concentration parameter (k) for the considered mixed dual-hop FSO-RF system.

$$J_4 = \sum_{\substack{l_1+l_2+l_3=N_1 \\ 0\le l_1,l_2,l_3\le N_1}} \binom{N_1}{l_1,l_2,l_3} \sum_{n=0}^{\infty} \frac{D_n(l_1,l_2,l_3)}{\Gamma\left(\frac{E}{r}\right)\left(\frac{E}{r}\right)} \left(\frac{\bar{\gamma}_{RD}}{m}\right)^{\frac{E}{r}+1} \Upsilon\left(\frac{mT_0}{\bar{\gamma}_{RD}}, u\right). \quad (21)$$

The derived expressions for J_i, $i \in \{1,2,3,4\}$ are substituted into (18) to obtain the PER for the considered system and is shown in (22) at the top of the next page.

D. Asymptotic OP Analysis

In order to obtain a deeper understanding of the considered system's performance, we derive the asymptotic expression for the OP at high SNR. Using the property of the lower incomplete Gamma function that $\Upsilon(z,c) \to 0$ as $z \to 0$, the OP of the RF link falls to zero at higher SNR values. As a result, only the S-R FSO communication link will dominate at high SNR. Further, in (16) it is noticed that only the first term in the summation corresponding to $n = 0$ will be significant at high SNR. Thus, the asymptotic OP is approximated as

$$P_{o,CC} \approx \sum_{\substack{l_1+l_2+l_3=N_1 \\ 0\le l_1,l_2,l_3\le N_1}} \binom{N_1}{l_1,l_2,l_3} \frac{D_0(l_1,l_2,l_3)(2^R-1)^{\frac{E}{r}}}{\Gamma\left(\frac{E}{r}\right)\left(\frac{E}{r}\right)\bar{\gamma}_{SR_r}^{\frac{E}{r}}}. \quad (23)$$

It is evident from (23) that $P_{out,CC} \propto (1/\bar{\gamma}_{SR_r})^{\frac{E}{r}}$ at large value of $\bar{\gamma}_{SR_r}$ and E consists of a, b, and ξ^2 with possible combinations of l_1, l_2, and l_3 with respect to N_1. Thus, the diversity gain is $N_1 \min\left\{\xi^2/r, a/r, b/r\right\}$.

Remark 3: It is interesting to observe the following:

- The diversity of the considered system is dependent only on the FSO link parameters and is independent of the RF link parameters.
- The number of transmission rounds, detection technique, turbulence parameters, and PE parameter influence the diversity of the considered system.

IV. Numerical Results and Discussion

In this section, we will discuss the analytical results presented in the preceding section. Some key system parameter values are R=1 bps/Hz, A_0=1, ξ=1.2, d_1=d_2=10m, M=128, ν=2.6, and (a=2.064; b=1.342). Unless otherwise stated, we assume light fog with link visibility and distance of 1 km on the S-R link [6], [7], [12, Eq. (3.68)]. We have generated 10^6 samples of the random variables for the simulation in MATLAB version R2021a.

Figure 2 (a) shows the OP versus SNR for the considered mixed dual-hop FSO-RF system, where (a=2.064; b=1.342), (a=2.296; b=1.822), and (a=2.902 ; b=2.51) represent strong, moderate, and weak AT, respectively. We consider generalized HD (r=1) and IM/DD (r=2) techniques on S-R hop and H-ARQ with CC protocol transmission rounds N_1=3 and N_2=2 with $\bar{\gamma}_{RD}$=50 dB. As we move from strong turbulence to weak turbulence scenario, the value of the OP performance reduces as the average SNR increases. Further, it can be noticed that the HD technique gives better outage performance compared to IM/DD technique. Moreover, we note that the OPs are 1.562×10^{-7} and 1.179×10^{-9} at $\bar{\gamma}_{SR_2}$=50 dB and $\bar{\gamma}_{SR_2}$=60 dB, respectively, for a=2.296, b=1.822, ξ=1.2, N_1=3, N_2=2, and r=2. Thus, the asymptotic slope is calculated as $\log_{10}(1.562 \times 10^{-7}) - \log_{10}(1.179 \times 10^{-9})$=2.12 $\approx N_1 \min\left\{\xi^2/r, a/r, b/r\right\}$=$N_1\xi^2/2$. Likewise, the asymptotic slopes can be calculated and verified for other curves, which validates the asymptotic slope analysis conducted in Section III.D. This asymptotic analysis is instrumental in revealing that the FSO system parameters are crucial for improving the overall OP performance; the RF system parameters do not play a dominant role in improving the diversity order. In the figure, we have also included the curves showing the effects of jitter and boresight (σ_x, σ_y)=$(4,4)$, (μ_x, μ_y)=$(6,6)$ that results into degradation of the OP performance of considered system.

Figure 2 (b) shows the effect of IRS reflector number on the OP of the considered cascaded system for for N_1=3 and various H-ARQ rounds on R-D link. We consider $\bar{\gamma}_{SR_1}$=45 dB and $\bar{\gamma}_{RD}$=25 dB on the S-R and R-D links, respectively. It can be seen that OP performance gets better with the increasing number of reflectors. Moreover, with increasing the H-ARQ transmission rounds, the OP performance improves. Using IRS elements and the H-ARQ protocol, we can compensate for the RF fading deterioration.

Figure 2 (c) indicates the OP as a function of k for $\bar{\gamma}_{SR_1}$=45 dB, $\bar{\gamma}_{RD}$=40 dB, and M=164 where parameter k is the concentration parameter of the von Mises distribution

This article has been accepted for publication in a future issue of this journal, but has not been fully edited. Content may change prior to final publication. Citation information: DOI 10.1109/LCOMM.2021.3129594, IEEE Communications Letters

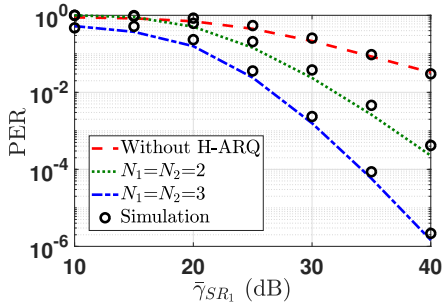

Fig. 3: Comparison of PER versus SNR under strong AT for H-ARQ with CC protocol and HD technique.

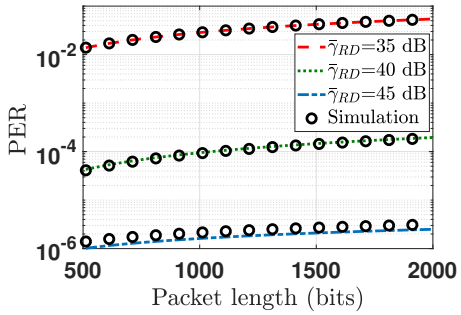

Fig. 4: Comparison of PER versus packet length under strong AT for H-ARQ with CC protocol and HD technique for $\bar{\gamma}_{SR_1}$=40 dB.

which reflects the accuracy of the phase error estimation [11]. It can be noticed that as parameter k increases, the OP performance enhances. Thus, the inclusion of IRS phase error in our analysis is essential for closely emulating practical system model.

The PER versus SNR performance has been plotted for various number of H-ARQ transmission rounds in Figure 3, where we consider the packet length of 1024 bits and $\bar{\gamma}_{RD}$=45 dB. It can be inferred that PER performance improves with the SNR on the FSO link. Moreover, the PER performance enhances as the H-ARQ transmission rounds increases. It can be observed that the RF fading, PE, and AT effect can be compensated using the H-ARQ protocol on both the links.

Figure 4 indicates PER versus packet length for different values of $\bar{\gamma}_{RD}$ and fixed $\bar{\gamma}_{SR_1}$=40 dB. It is observed that as packet length increases, the PER performance slowly degrades and then saturates for higher packet lengths. Moreover, it is also seen that on increasing $\bar{\gamma}_{RD}$ from 35 dB to 45 dB, the PER improves. From this figure, it can be observed that the increase in packet length does not significantly change the PER as the average SNR improves.

Figure 5 demonstrates the comparative analysis of OP versus SNR (dB) for the proposed system with respect to the previous works in literature on mixed FSO-RF systems [1], [18]. The system parameters used for obtaining the curves are: a=2.064, b=1.342, $\bar{\gamma}_{RD}$=50, and d_1=d_2=10m. For the traditional mixed FSO-RF system, we assume that the distance between R to D is 20 m. From the figure, it is evident that the proposed system outperforms the traditional mixed FSO-RF communication systems without IRS and the mixed FSO-RF communication systems with IRS but without H-ARQ in terms of OP [1], [18].

V. Conclusions

In this letter, we investigated the performance of a mixed dual-hop FSO-RF system using IRS with phase error on the R-D link and H-ARQ protocol over both hops. We derive novel closed-form expressions of OP and PER for the considered system. Useful design insights into the system performance are obtained through the diversity analysis. The presented results comprehensively capture the impact of various system parameters such as AT, PEs, number of IRS reflectors, concentration parameter, H-ARQ rounds, and detection techniques on the outage and PER that are critical for the design of such mixed FSO-RF systems.

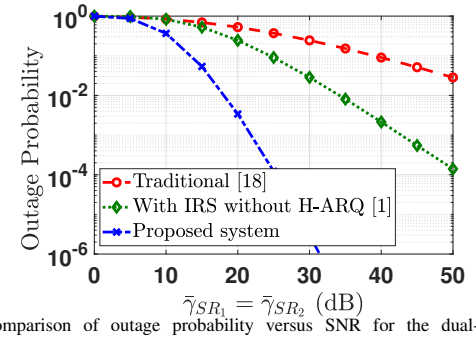

Fig. 5: Comparison of outage probability versus SNR for the dual-hop FSO-RF communication systems.

References

[1] L. Yang *et al.*, "Mixed dual-hop FSO-RF communication systems through reconfigurable intelligent surface," *IEEE Commun. Lett.*, vol. 24, no. 7, pp. 1558–1562, 2020.

[2] Y. Ai *et al.*, "Secrecy enhancement of rf backhaul system with parallel fso communication link," *Optics Commun.*, vol. 475, p. 126193, 2020.

[3] A. Mathur *et al.*, "Performance of hybrid ARQ over power line communications channels," in *2020 IEEE 91st . Veh. Technol. Conference (VTC2020-Spring)*, 2020, pp. 1–6.

[4] S. Ge *et al.*, "Packet error rate analysis and power allocation for CC-HARQ over Rayleigh fading channels," *IEEE Commun. Lett.*, vol. 18, no. 8, pp. 1467–1470, 2014.

[5] Y. Xi *et al.*, "A general upper bound to evaluate packet error rate over quasi-static fading channels," *IEEE Trans. Wireless Commun.*, vol. 10, no. 5, pp. 1373–1377, 2011.

[6] G. D. Verma *et al.*, "Performance improvement of FSO communication systems using hybrid-ARQ protocols," *Appl. Opt.*, vol. 60, no. 19, pp. 5553–5563, Jul 2021.

[7] A. Sikri *et al.*, "Reconfigurable intelligent surface for mixed FSO-RF systems with co-channel interference," *IEEE Commun. Lett.*, vol. 25, no. 5, pp. 1605–1609, 2021.

[8] Y. Ai *et al.*, "On hybrid-ARQ-based intelligent reflecting surface-assisted communication system," *arXiv preprint arXiv:2009.10776*, 2020.

[9] V. Jamali *et al.*, "Intelligent surface-aided transmitter architectures for millimeter-wave ultra massive MIMO systems," *IEEE Open J. Commun. Soc.*, vol. 2, pp. 144–167, 2021.

[10] M. R. Bhatnagar *et al.*, "Performance analysis of Gamma–Gamma fading FSO MIMO links with pointing errors," *J. Lightw. Technol.*, vol. 34, no. 9, pp. 2158–2169, 2016.

[11] M. A. Badiu *et al.*, "Communication through a large reflecting surface with phase errors," *IEEE Wireless Commun. Lett.*, vol. 9, no. 2, pp. 184–188, 2020.

[12] Z. Ghassemlooy *et al.*, *Optical wireless communications: system and channel modelling with Matlab®*. CRC press, 2019.

[13] F. Yang *et al.*, "Free-space optical communication with nonzero boresight pointing errors," *IEEE Trans. Commun.*, vol. 62, no. 2, pp. 713–725, February 2014.

[14] I. S. Gradshteyn *et al.*, *Table of integrals, series, and products*, 7th ed. Elsevier/Academic Press, Amsterdam, 2007.

[15] K. V. Mardia *et al.*, *Directional statistics*. John Wiley & Sons, 2009, vol. 494.

[16] S. Liu *et al.*, "On the throughput and optimal packet length of an uncoded ARQ system over slow Rayleigh fading channels," *IEEE Commun. Lett.*, vol. 16, no. 8, pp. 1173–1175, 2012.

[17] A. P. Prudnikov *et al.*, *Integrals and Series of Special Functions. Vol.2*. RUS: Science, 1983.

[18] E. Zedini *et al.*, "Performance analysis of mixed Nakagami-*m* and Gamma–Gamma dual-hop fso transmission systems," *IEEE Photon. J.*, vol. 7, no. 1, pp. 1–20, 2015.